JOURNAL OF MATERIALS SCIENCE 33 (1998) 1737–1744

Influence of increased nitriding temperatures on the hardness profile of low-alloy steels

R. S. E. SCHNEIDER, H. HIEBLER
Department of Ferrous Metallurgy, Montanuniversität Leoben, Franz-Josef-Strasse 18, A-8700 Leoben, Austria
E-mail: eisen@unileoben.ac.at

Gaseous nitriding at temperatures of 550, 590 and 630 °C (823, 863 and 903 K), was applied for various times to three different steels (16 MnCr 5, 30 CrMoV 9 and 34 CrAlNi 7). In a second stage, two or three of these temperatures were combined to investigate the effects of step-nitriding. Hardness profiles were measured with low-load hardness testing to determine the growth of the case depth after nitriding. Microhardness testing was carried out on selected samples to investigate the hardness profile at the transition from the compound to the diffusion layer, including the transformed austenite layer. Effects, possibilities and limits of an application at higher than usual nitriding temperatures are discussed, emphasizing especially the effects of precipitation ageing and the influence of the porous zone. © *1998 Chapman & Hall*

1. Introduction

Higher nitriding temperatures have gained increasing attention in recent times [1–8]. While usual nitriding conditions have faced comprehensive investigations in the past, very little is still known about the various influences and possibilities at higher temperatures. Time and temperature represent the main factors which determine the hardness profile on nitrided steels with certain composition. Possible shorter treatment times are faced with decreasing hardness and the arising of an austenitic layer during nitriding. Because of this, the upper limits of industrial applied nitriding temperatures usually range between 550 and 600 °C, depending also on the process.

The application of nitriding in steps of rising temperature provides the possibility to combine high surface hardness with increased depth of nitriding. Stable precipitated nitrides can retain the hardness in the surface area when a higher temperature is applied to increase the diffusion towards the centre in the second stage of the process. In the present investigation, this process was applied to three typical steels used for nitriding (16 MnCr 5, 30 CrMoV 9 and 34 CrAlNi 7). The temperatures were up to 630 °C in systematic combinations. Thus, it can be shown that it is possible to achieve a substantial hardening effect at higher than usual process temperatures.

2. Experimental procedure

2.1. Specimens and preparation

Specimens used for nitriding were quarter segments of discs 40 mm in diameter and 10 mm thick. The chemical composition and the corresponding material number is given in Table I.

The specimens were cut from round bars, hardened in oil at 860 °C, annealed for 1 h at 650 °C and polished. After grinding with # 1200 emery paper, all specimens were cleaned in alcohol.

2.2. Nitriding procedure

The experimental apparatus consists of a horizontal tube furnace with an inner diameter of 65 mm and 600 mm in length, a retort made of Inconel 600 and a gas analytical equipment.

To achieve rapid heating, the furnace was heated to the operating temperature prior to the experiment. The charging of the retort took place under a pure ammonia atmosphere. Detailed information about the time–temperature profile can be seen in Fig. 1, which describes a typical two-step nitriding process. The temperature measurements of the furnace and inside the treatment chamber were realized with Ni–CrNi thermocouples. To determine the duration of the treatment in total, t_{total}, or a single step, t_1, t_2, it was necessary to set a starting point from which the time is counted. In all experiments, the first 15 min (a, heating) and the cooling period after the removal of the retort from the furnace (b, cooling) were not counted as a part of the treatment time. The change from one temperature step to the next was determined from the onset of heating.

To control the chemical potential of the nitriding atmosphere, a continuous infrared gas analysis was applied, measuring the ammonia content of the exhaust gas. As determined by the ammonia decomposition, the nitriding potential $K_H = p_{(NH_3)}/p^{3/2}_{(H_2)}$ was kept between 3.5 and 4.

TABLE I Material number, chemical composition and austenizing temperature in nitrided layers ($A_{cl(nitrided)}$) of the investigated materials

	Material number	C	Si	Mn	P	S	Cr	Al	Ni	Mo	V	$A_{cl(nitrided)}$ temperature (°C)
16 MnCr 5	1.7131	0.17	0.29	1.29	0.009	0.034	0.94	0.03	0.12	0.05	0.01	605–610
30 CrMoV 9	1.7707	0.30	0.27	0.43	0.016	0.020	2.33	0.01	0.09	0.17	0.13	615–620
34 CrAlNi 7	1.8550	0.30	0.29	0.50	0.009	0.018	1.56	1.04	0.90	0.17	0.01	640–650

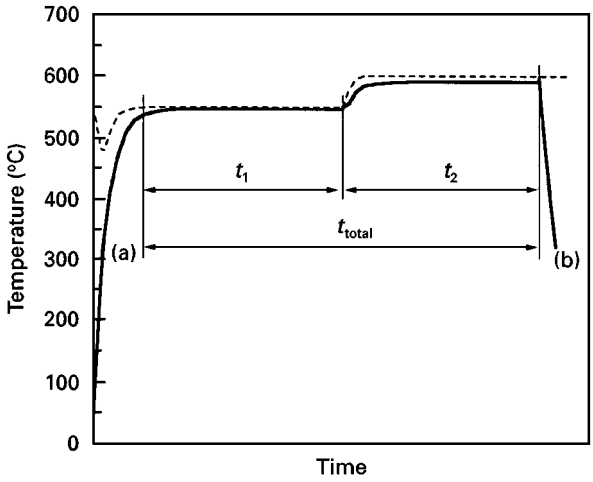

Figure 1 Schematic time–temperature sketch for experiments with two-step nitriding at 550–590 °C and various nitriding times. (– – –) Furnace temperature, (—) retort temperature (treatment chamber). (a) Heating (15 min), (b) cooling.

2.3. Metallography

For measurement of the hardness profile, low-load hardness and microhardness testing were carried out on transverse microsections. While low-load hardness testing was performed under 500 g load (HV 0.5) to determine the complete hardness profile, microhardness testing with 50 g (HV 0.05) was applied to measure the hardness at the transition from the compound layer to the diffusion layer, and respectively also in the transformed austenitic layer.

As a result of the hardness profiles it was possible to determine the effective case depth after nitriding. Based on the systematic variation of the time and temperature parameters, the growth kinetics of the depth of nitration could be investigated. To obtain a uniform base for this measurement, the limiting hardness was fixed with 50 HV 0.5 above the maximum core hardness of all samples from the same alloy. Etching for morphological investigations was performed for 3 s in 3% alcoholic nitric acid.

Prior to the investigations of the hardness profile, a couple of experiments were made to determine the temperature of the first appearance of the austenite layer. Detailed results can be seen in Table I, and show that one steel (34 CrAlNi 7) was still free of such a layer at the highest applied temperature (630 °C) of the hardness investigations. These results correspond well to those of Schröter *et al.* [9] for similar steels.

2.4. X-ray diffraction

Three selected samples, one of each steel, which were step-nitrided up to 630 °C, were scanned for phase identification. Prior to the scans, the samples were ground and polished to an angle of about 2° towards the original surface. In this way it was possible to perform phase identification with CrK_α radiation for all layers in one scan.

3. Results

3.1. Effective case depth after nitriding at various temperatures

Because systematic investigations of the development of case depths after nitriding at higher temperatures are rare and not available for many materials [4, 5, 8, 10], it was necessary to perform a prior investigation on that topic. In the first stage of the experiments, the hardness profiles after nitriding at single temperatures were measured, and the development of the case depths was determined. Three different temperatures were applied: 550 °C, which represents a typical nitriding temperature; 590 °C, which is at the upper limit of today's industrial applied nitriding temperatures; 630 °C, to investigate the possibilities of increased nitriding temperatures.

Typical results can be seen in Fig. 2a–c for the temperature of 630 °C and all three steels, thereby also showing the main effects of high nitriding temperatures on the hardness profile. For comparison, the 550 °C/4 h and 550 °C/16 h hardness profiles are included in the diagrams. The known effects of decreasing hardness and higher case depths after nitriding could be found in all three materials. After more than 8 h nitriding at 630 °C the hardness profiles of the steels 16 MnCr 5 and 30 CrMoV 9 show no further gain, or even a decrease, in case depth compared to the 550 °C/16 h and 630 °C/8 h experiments.

All three steels show a more or less sharp decrease in hardness in the first 0.1 mm. While the hardness profiles of the steels 16 MnCr 5 and 30 CrMoV 9 have a continuous decrease towards the centre, the aluminium alloyed steel has a plateau-shaped profile with a rather sharp drop at the transition to the core hardness. This effect was described in detail by Wiedemann *et al.* [11] and is based on the formation of aluminium nitrides.

A dropping hardness profile at longer treatment times can be seen clearly for the steel 30 CrMoV 9, leading to a much decreased hardness profile of the 16 h experiment compared to the 8 h experiment (Fig. 2b). Similar behaviour, but not so typically developed, was also observed at steel 16 MnCr 5.

The growth of the effective case depth after nitriding for all three temperatures can be drawn from Fig. 3a–c. In this figure, the limitation in case depth

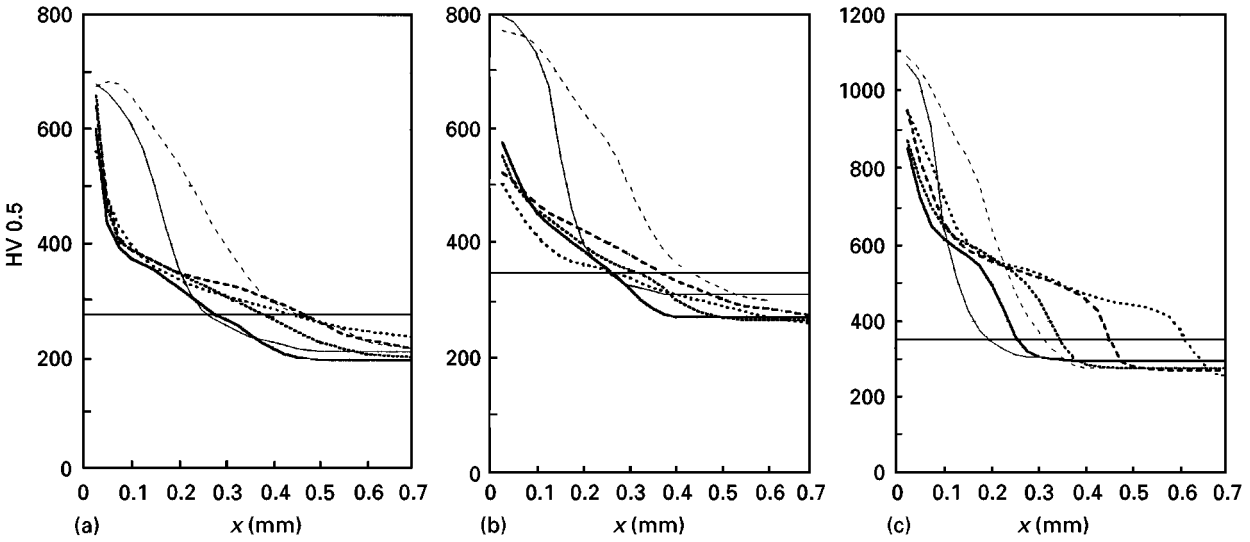

Figure 2 Hardness profiles of (a) 16 MnCr 5, (b) 30 CrMoV 9, (c) 34 CrAlNi 7, after nitriding at 630 °C for (—) 2 h, (·····) 4 h, (- - -) 8 h and (· · ·) 16 h. Also shown are the results for 550 °C, (—) 4 h and (- - -) 16 h.

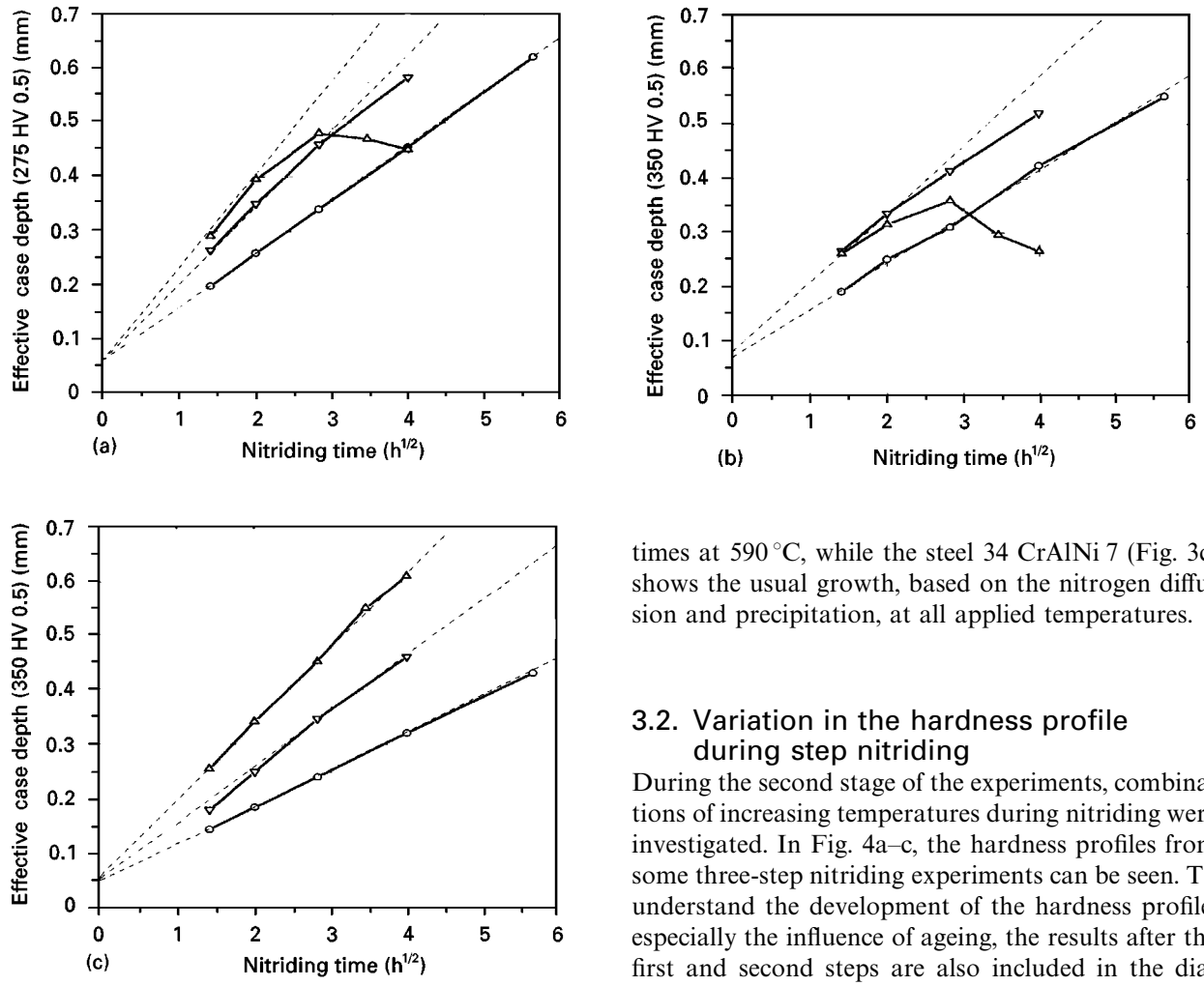

Figure 3 Effective case depth growth during nitriding at different temperatures: (a) 16 MnCr 5, (b) 30 CrMoV 9, (c) 34 CrAlNi 7. (○) 550 °C, (▽) 590 °C, (△) 630 °C.

growth for the steels 16 MnCr 5 and 30 CrMoV 9 at 630 °C can be very clearly seen. For these steels it also turned out that they have increased deviations from the square root growth law (- - - -) at longer nitriding times at 590 °C, while the steel 34 CrAlNi 7 (Fig. 3c) shows the usual growth, based on the nitrogen diffusion and precipitation, at all applied temperatures.

3.2. Variation in the hardness profile during step nitriding

During the second stage of the experiments, combinations of increasing temperatures during nitriding were investigated. In Fig. 4a–c, the hardness profiles from some three-step nitriding experiments can be seen. To understand the development of the hardness profile, especially the influence of ageing, the results after the first and second steps are also included in the diagrams. For further comparisons, the 550 °C/16 h and the 630 °C/16 h hardness profiles are also shown.

Increased nitriding temperatures show a strong effect on the steels 16 MnCr 5 and 30 CrMoV 9. The high hardness in the near-surface regions collapses to much lower values when a higher nitriding temperature is applied in the second step. The even higher temperature of the third step leads to a further flattening of the hardness profile. In comparison with the hardness profile of the pure 630 °C/16 h experiment,

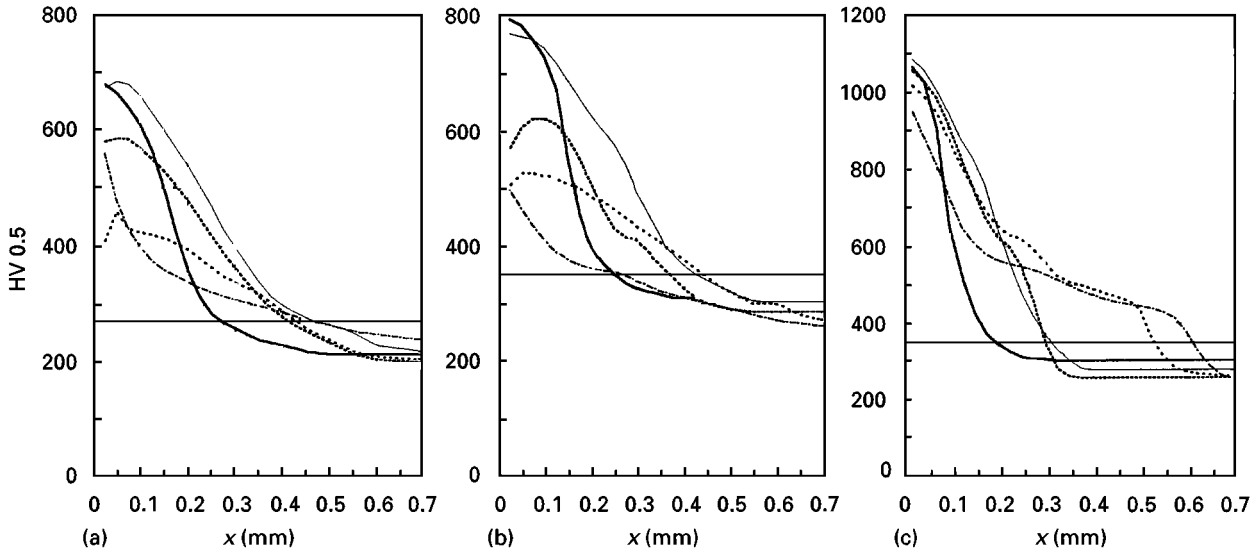

Figure 4 Hardness profiles after step nitriding at 550–590–630 °C: (a) 16 MnCr 5, (b) 30 CrMoV 9, (c) 34 CrAlNi 7. (—) 550 °C/4 h, (- - -) 550 °C/4 h + 590 °C/4 h, (···) 550 °C/4 h + 590 °C/4 h + 630 °C/8 h, (—) 550 °C/16 h, (–·–) 630 °C/16 h.

the hardness values after step nitriding remain higher (Fig. 4a,b), the 550 °C/16 h profile is well above and shows nearly the same case depth after nitriding.

In contrast, the hardness profile of the steel 34 CrAlNi 7 develops in a very advantageous way. The high hardness in near-surface regions, resulting from the first nitriding step at 550 °C, remains fully developed after both the second and third steps. Thereby the final hardness profile remains well above those of the plain 630 °C/16 h experiment, just showing a slightly reduced case depth. In comparison with the 550 °C/16 h profile, the near-surface hardness is approximately the same, while the case depth after nitriding has nearly doubled.

3.3. Effective case depth after step-nitriding with different temperature combinations

To compare the results of the step-nitriding variations, the case depths after nitriding at only one constant temperature are included in Fig. 5a–c as thin lines. For all experiments, the case depths of step-nitriding were higher than those after nitriding exclusively at 550 °C for the same duration. For the steel 16 MnCr 5, all variations starting with 2 h at 550 °C and lasting for 8 h gave similar results, reaching approximately the case depth of the 590 °C experiments. The three-temperature experiment starting with 4 h at 550 °C and 4 h at 590 °C in the second step, principally shows a similar behaviour, and even crosses the case depth line after nitriding solely at 630 °C. The additional gain in the third step at 630 °C for 8 h has a lower growth rate than the plain 550 °C experiments.

The results of the steel 30 CrMoV 9 basically show a similar development, but are less uniform. In particular, combinations with 630 °C in the second or third step result in a very limited gain in case depth compared to the 550 °C experiments. This gain is almost completely lost in the experiment with 8 h at 630 °C in the third step, but it is still much higher compared to the sharply shrinking results of nitriding solely at 630 °C.

The best results again could be found for steel 34 CrAlNi 7. Case depths for all temperature combinations approach the results of the case depths after nitriding at the highest applied temperature. No degeneration in the growth rate during the highest temperature step could be observed.

3.4. Hardness profiles at the transition from the compound layer to the diffusion layer

To observe the influence of higher nitriding temperatures on the hardness profile at the transition from the compound layer to the diffusion layer, and respectively also inside the transformed austenitic layer, microhardness investigations were performed on six selected samples. The first series was measured on specimens treated for 16 h at 630 °C, taking one sample from each steel (Fig. 6). The second series, also comprising samples from each of the steels, was nitrided in a temperature combination of 550 + 590 + 630 °C (Fig. 7). Hardness values measured with HV 0.05 microhardness testing correspond well with the results of low-load hardness testing at 25, 50, 75, 100 and 125 μm.

Because the aluminium alloyed steel (34 CrAlNi 7) experiences no formation of an austenitic layer during nitriding at temperatures up to 630 °C, there is a direct transition from the compound layer to the precipitation-hardened diffusion layer. Both samples (Figs 6 and 7) showed their maximum hardness at the inner part of the compound layer in the transition area. While there were no sharp transitions in either profile, the hardness values of the step-nitrided sample was generally about 100 HV 0.05 higher.

The hardness profiles of the other two steels (16 MnCr 5, 30 Cr MoV 9) are dominated by the hardness peak inside the transformed former austenitic layer. This hardness peak is more dominant in

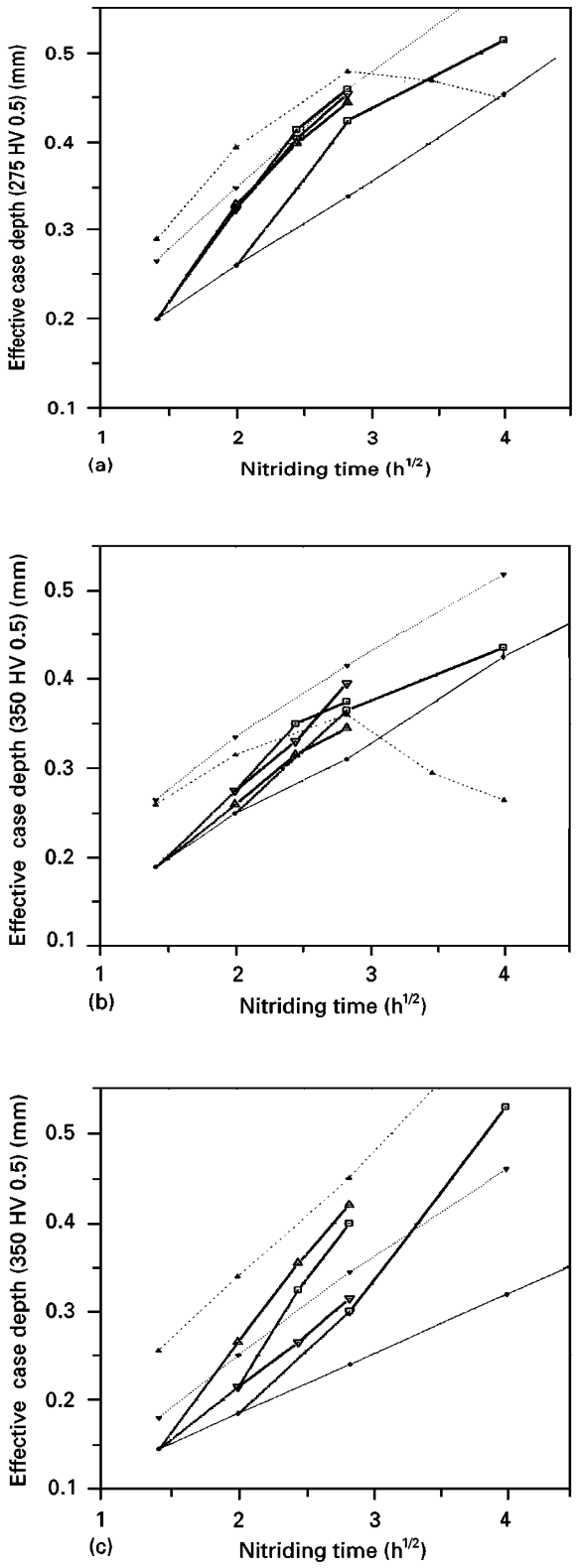

Figure 5 Effective case depth growth during step-nitriding: (a) 16 MnCr 5, (b) 30 CrMoV 9, (c) 34 CrAlNi 7. (●) 550 °C, (▼) 590 °C, (▲) 630 °C, (▽) 550 + 590 °C, (△) 550 + 630 °C, (□) 550 + 590 + 630 °C.

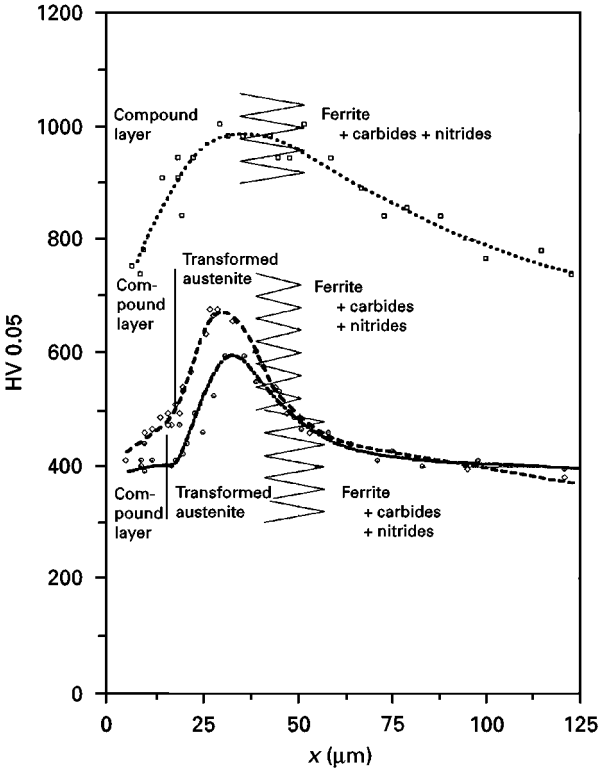

Figure 6 Hardness profiles at the transition from the compound layer to the diffusion layer for the steels (---) 16 MnCr 5, (—) 30 CrMoV 9 and (···) 34 CrAlNi 7 after nitriding at 630 °C for 16 h.

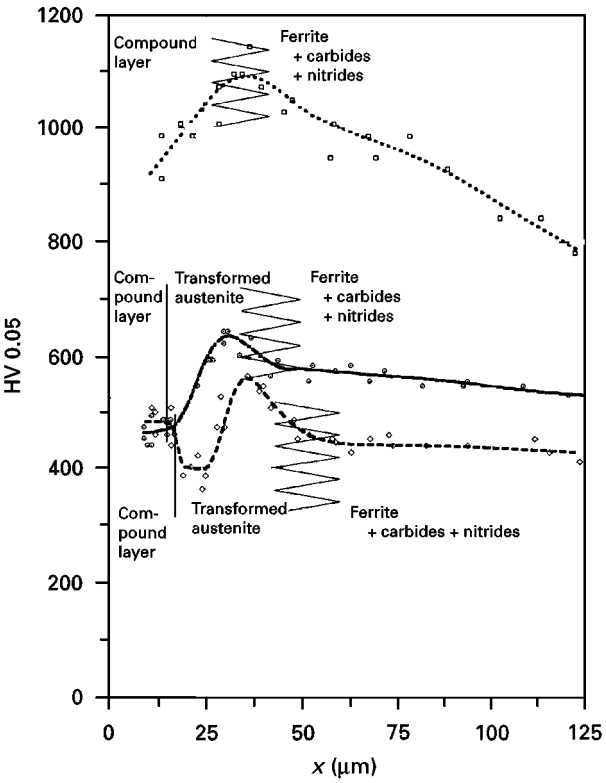

Figure 7 Hardness profiles at the transition from the compound layer to the diffusion layer for the steels (---) 16 MnCr 5, (—) 30 CrMoV 9 and (···) 34 CrAlNi 7 after three-step nitriding at 550 °C (4 h) + 590 °C (4 h) + 630 °C (8 h).

the 630 °C/16 h samples (Fig. 6), where the compound layer hardness, as well as the diffusion layer hardness, are comparatively low and at similar values. It is important to realize that the maximum hardness is reached in the middle of the transformed austenite layer, and the hardness curve is already dropping inside this layer towards the compound layer. The transition from the transformed austenite layer to the diffusion layer is gradual, comprising a zone where precipitation-hardened ferrite and transformed austenite are mixed.

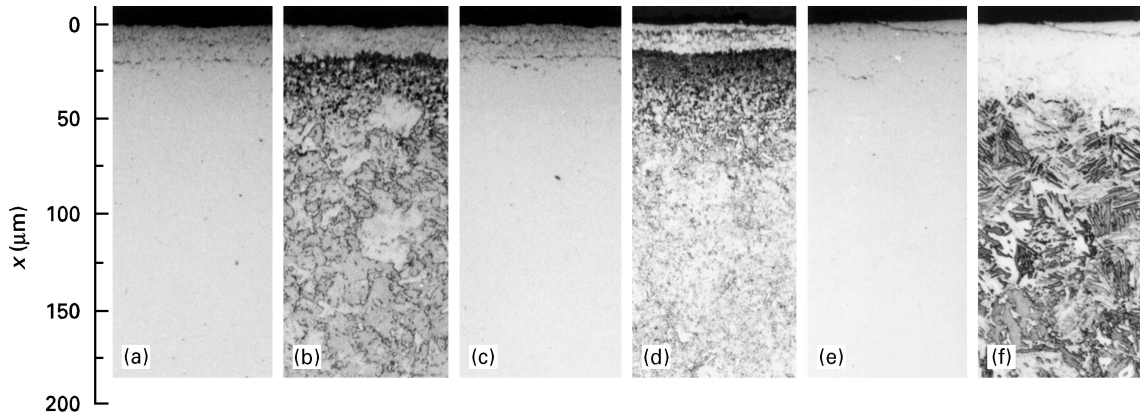

Figure 8 Photomicrographs of the transition from the compound layer to the diffusion layer for the steels (a,b) 16 MnCr 5, (c, d) 30 CrMoV 9 and (e, f) 34 CrAlNi 7, after nitriding at 630 °C for 16 h; (b, d, f) etched for 3 s in nital.

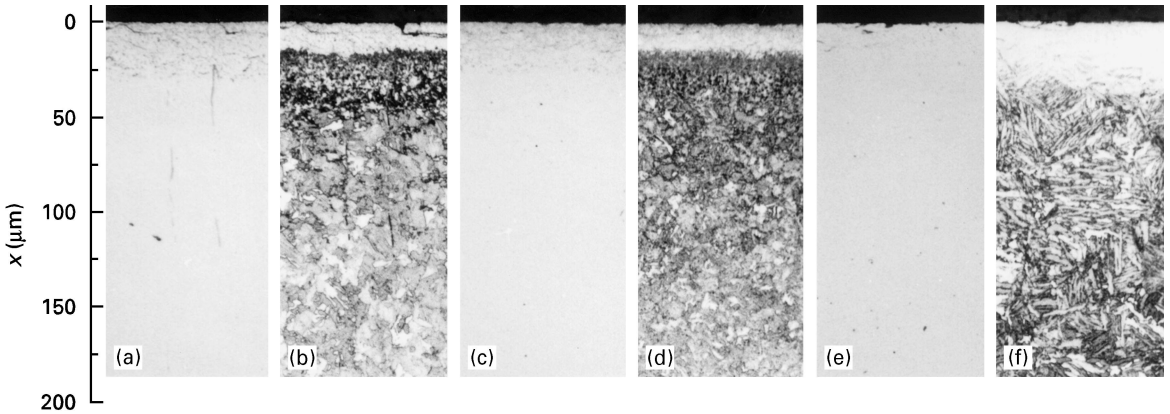

Figure 9 Photomicrographs of the transition from the compound layer to the diffusion layer for the steels (a, b) 16 MnCr 5, (c, d) 30 CrMoV 9 and (e, f) 34 CrAlNi 7, after three-step nitriding at 550 °C (4 h) + 590 °C (4 h) + 630 °C (8 h); (b,d,f) etched for 3 s in nital.

After step-nitriding, the hardness profile for steel 30 CrMoV 9 is similar but on a higher hardness level. The hardness gain is the biggest in the diffusion layer, thus making the drop on the right side of the maximum rather slight.

The hardness profile for the steel 16 MnCr 5 is substantially different in the step-nitrided sample. While the hardness values of the diffusion layer rose slightly or remained about the same inside the compound layer, there was a substantial drop in the transformed austenite layer compared to the 630 °C/16 h hardness profile. This includes a reduction in the maximum hardness of about 100 HV 0.05 as well as a hardness minimum in the outer zone of the transformed austenite layer.

3.5. Morphological investigation

To observe the composition and the influence of the different layers and of the porous zone, optical metallographic investigations were performed. Results for all three steels of the 630 °C/16 h experiments are presented in Fig. 8a–f and for the 550 + 590 + 630 °C step-nitriding experiments in Fig. 9a–f.

The left-hand pictures show the unetched cross-section with the porous zone clearly visible. The right-hand picture, taken from the same spot, show the microstructure from the surface to the diffusion layer after etching. Thus, the white layer is the compound layer, partly containing cracks in near-surface regions. Figs 8b and d and 9b and d (16 MnCr 5, 30 CrMoV 9) show the partly transformed austenite layer adjacent to the compound layer. This layer can be divided into a fine outer part and a coarse inner part which passes into the diffusion layer. The outer fine-structured part corresponds well with the extension of the porous zone in the corresponding pictures on the left (Figs 8a, c and 9a, c). In contrast, the steel 34 CrAlNi 7 (Figs 8e, f and 9e, f) has no such layer and the porous zone is limited to the outer rim of the compound layer.

3.6. Phase analysis by X-ray diffraction

All three steels showed clear peaks of ferrite (α-iron) and γ′-nitride (Fe_4N). ε-nitride was clearly detected for the steel 34 CrAlNi 7, but was also found in minor quantities in the other two steels. Austenite (= residual austenite) was easy to detect in the sample of the steel 30 CrMoV 9. The other two steels showed just very weak signs of austenite. This is especially interesting for the steel 34 CrAlNi 7, which has no visible extra layer between the compound and the diffusion layer. The austenite, therefore, has to be explained by

local transformation to austenite based on segregations. This is likely, as the applied temperature was just about 10 °C below the temperature where a transformed austenite layer was detected by optical metallography.

4. Discussion

4.1. Effects of higher nitriding temperatures

Owing to the heating under an ammonia atmosphere, the nitriding process begins at a substantially lower temperature than the final applied temperature. During these first minutes, very fine nitrides are formed in near-surface regions, providing a high precipitation hardness in that area. Depending on the stability of these nitrides, the high hardness remains more or less after long-term nitriding at much higher temperatures. This effect is especially strong in the steel 34 CrAlNi 7 (Fig. 2c). Both other steels additionally experienced a phase transformation of the austenitic layer to bainite and residual austenite, which results in a hard sublayer below the surface. Detailed information is given later.

The development of the hardness profile is mainly determined by the size and stability of the precipitated (carbo-)nitrides. At higher nitriding temperature, rather coarse nitrides are formed, resulting in a limited gain in hardness. There is also an additional ageing effect after longer nitriding times. All these lead to flat hardness profiles with a limited gain in case depth compared to normal nitriding temperatures. For the steels 16 MnCr 5 and 30 CrMoV 9, the ageing effect reduces the faster growth in case depth with higher nitriding temperatures after longer treatment times.

It can be seen from Fig. 3 that higher nitriding temperatures can improve case depth, but there seems to be a maximum temperature where ageing effects limit further growth. This maximum temperature depends on the alloying elements and is different for all three steels investigated. Steel 34 CrAlNi 7 showed the best results and was free of substantial ageing effects at all investigated temperatures. In comparison with the results of Brandis [12] at 500–550 °C, there is a good correspondence in case depth.

4.2. Effects of the step-nitriding treatment

As already reported about the influence of low nitriding temperatures during the heating, the effect of ageing is easier to observe here. During the low-temperature step at the beginning, many fine precipitates are formed in near-surface regions. After applying higher temperatures in the second and third steps, ageing effects reduce the hardness profile. These are especially strong in steels 16 MnCr 5 and 30 CrMoV 9, although the steel 34 CrAlNi 7 again shows no such ageing effect.

Even if such ageing effects occur, the remaining hardness is still higher compared to a treatment solely at the higher temperature, showing that step nitriding can increase hardness values substantially even at high nitriding temperatures.

The reason for the advantageous behaviour of steel 34 CrAlNi 7 can be found in the stability of the precipitation of aluminium-containing nitrides [4, 5, 13]. In comparison to chromium, molybdenum, vanadium and manganese, aluminium usually forms no carbides, and therefore also no large carbonitrides with limited contribution to the increasing hardness. Comprehensive investigations on that topic and the influence of tempering can be found elsewhere [14, 15]. These fine aluminium nitrides, once formed, seem to remain stable even after longer treatment time at higher temperatures, thereby keeping the hardness once achieved in the first lower temperature nitriding step.

4.3. Effects of the transformed austenite layer

While the hardness profile in the compound and the diffusion layer is the result of the nitriding conditions during the whole treatment, the hardness of the former austenite layer is determined by the cooling conditions after the nitriding process. Basically there are three possibilities [2]:

(i) braunite, corresponding to pearlite after slow cooling, or tempering at above 450 °C after quenching;

(ii) bainite (with residual austenite), after faster cooling, or tempering at about 300 °C after quenching;

(iii) austenite or martensite, after quenching.

Therefore, results cannot be compared generally. For all experiments of this investigation, the cooling conditions were the same, because the retort was removed from the furnace and cooled in air. More detailed information on that topic can be found elsewhere [16–18]. The importance of a hard sublayer as a support for the compound layer, especially for steels with no or low contents of alloying elements, has been described [18, 19].

The difference in the hardness profiles (Figs 6 and 7) of steel 30 CrMoV 9 can be well explained. The increased hardness of the diffusion layer (ferrite + carbides + nitrides) after step nitriding is based on precipitate formation at lower temperatures. Similar effects can be regarded as the reason for the slight increase in the maximum hardness inside the transformed austenite layer, as well as in the compound layer.

While the effects seem to be similar, but less strong, in the diffusion layer and the compound layer (slight increase in hardness) of the steel 16 MnCr 5, the transformed austenite layer shows a quite different behaviour. The reasons for the substantial lower maximum hardness after step-nitriding may be found in an investigation of the precipitation and redissolution of the formed nitrides and carbides in austenite.

A drop in hardness inside the transformed austenite layer towards the compound layer is generally regarded as the result of residual austenite [3, 8, 20]. A conclusion from the optical investigation (Figs 8, 9) of these samples, is that the drop seems to be also effected by the result of a porous zone that stretches into the transformed austenite layer. Such pore formation and its thermodynamical cause is well summarized by Mittemeijer and Slycke [21]. This porous zone should be especially considered for the steel 16 MnCr 5, which showed just a very small content of austenite in the X-ray diffraction investigation. Thus,

the strong and deep porous zone can be considered as the main reason for the hardness minimum in the transformed austenite after step-nitriding of that steel.

5. Conclusions

Nitriding at higher temperatures promises the possibility to achieve applicable results at reduced treatment times. To determine a maximum temperature, different factors from the application via the steel composition to the detailed treatment parameters, have to be considered and optimized. No rule can be given, but several aspects were found to be of main importance.

1. Step-nitriding is a useful method to achieve a substantial surface hardness in combination with increased case depths after nitriding also at higher temperatures.

2. It could be found that maximum nitriding temperatures strongly depend on the steel composition. The aluminium-alloyed steel proved that a surface hardness of 1000 HV 0.5 is possible even at temperatures well above 600 °C.

3. Because of ageing effects, non-aluminium-containing steels experience a substantial decrease in hardness over the treatment time.

4. The former austenitic layer proved to be a hard sublayer if transformed at least partly into a bainitic structure and cannot generally be seen as a weak point.

5. The development of the porous zone has a substantial effect on the hardness profile in the compound and outer bainite layer.

Further investigations will be necessary to specify all influences, especially on the formation of the porous zone, and to find a better optimized process.

Acknowledgements

The authors thank Professor B. Ortner (Institute for Metallphysiks, MU-Leoben) for the X-ray diffraction measurements.

References

1. R. HOFFMANN, B. EDENHOFER, F. HOFFMANN, H. MALLENER, S. PAKRASI, W. SCHRÖTER and G. WAHL, *Härterei-Tech. Mitt.* **49** (1994) 319.
2. *Idem*, *ibid.* **49** (1994) 384.
3. Y. M. LAKHTIN, *Metalloved. Term. Obrab. Met.* **February** (1991) 25.
4. N. ISHIKAWA, T. SHIRAGA, K. SATO, M. ISHIGURO, H. KABASAWA and Y. KUWAHARA, *Tetsu to Hagane* **82** (1996) 66.
5. T. SHIRAGA, N. ISHIKAWA, M. ISHIGURO, H. KABASAWA and Y. KUWAHARA, *NKK Technical Rev.* **75** (1996) 19.
6. X. YANG, C. KONG and Y. QIAO, in "Proceedings of the 2nd International Conference on Carburizing and Nitriding with Atmospheres", edited by J. Grosch, J. Morrel and M. Schneider (ASM International, Materials Park, OH, 1995) p. 391.
7. K. MÄDLER, W. BERGMANN and D. DENGEL, *Härterei-Tech. Mitt.* **51** (1996) 338.
8. N. YASUMARU, *Mater. Trans. JIM* **33** (1992) 7.
9. W. SCHRÖTER, M. MATTMÜLLER, E.-K. FEHR and S. HOPPE, in "Tagungsband Nitrieren und Nitrocarburieren", edited by E. J. Mittemeijer and J. Grosch (Arbeitsgen. Wärmebehandlung und Werkstoff-Technik, Darmstadt, 1991).
10. B. EDENHOFER and H. TRENKLER, *Härterei-Tech. Mitt.* **35** (1980) 220.
11. R. WIEDEMANN, H. OETTEL and D. BERGENER, *ibid.* **46** (1991) 301.
12. H. BRANDIS, *Thyssen Edelst. Techn. Ber.* **12** (1986) 164.
13. R. S. E. SCHNEIDER and H. HIEBLER, *Härterei-Tech. Mitt.* **52** (1997) 371.
14. C. C. HODGSON and H. G. BARON, *J. Iron Steel Inst.* **182** (1965) 256.
15. G. SCAVINO, M. ROSSO, G. UMBERTALLI and A. BAZAROTTI, *Int. J. Mater. Prod. Technol.* **8** (1993) 290.
16. T. BELL, *Härterei-Tech. Mitt.* **30** (1975) 161.
17. *Idem*, *J. Iron Steel Inst.* **206** (1968) 1017.
18. S. PAKRASI, *Härterei-Tech. Mitt.* **43** (1988) 365.
19. F. K. CHERRY, *Heat Treatment Metals* **1987.1** (1987) 1.
20. T. BELL, M. KILANI and G. MUNSTERMANN, *ibid.* **1987.2** (1987) 47.
21. E. J. MITTEMEIJER and J. T. SLYCKE, *Surf. Engng* **12** (1996) 152.

Received 6 May
and accepted 27 November 1997